INSTITUTE OF PHYSICS PUBLISHING PHYSICS IN MEDICINE AND BIOLOGY

Phys. Med. Biol. **51** (2006) 1347–1360 doi:10.1088/0031-9155/51/5/022

Magnetogastrographic detection of gastric electrical response activity in humans

Andrei Irimia[1], **William O Richards**[2] **and L Alan Bradshaw**[1,2]

[1] Living State Physics Laboratories, Department of Physics and Astronomy, Vanderbilt University, Nashville, TN 37235, USA
[2] Department of Surgery, Vanderbilt University School of Medicine, Nashville, TN 37235, USA

E-mail: andrei.irimia@vanderbilt.edu

Received 12 October 2005, in final form 23 December 2005
Published 15 February 2006
Online at stacks.iop.org/PMB/51/1347

Abstract

The detection and characterization of gastric electrical activity has important clinical applications, including the early diagnosis of gastric diseases in humans. In mammals, this phenomenon has two important features: an electrical control activity (ECA) that manifests itself as an electric slow wave (with a frequency of 3 cycles per minute in humans) and an electrical response activity (ERA) that is characterized by spiking potentials during the plateau phase of the ECA. Whereas the ECA has been recorded in humans both invasively and non-invasively (magnetogastrography—MGG), the ERA has never been detected non-invasively in humans before. In this paper, we report on our progress towards the non-invasive detection of ERA from the human stomach using a procedure that involves the application of principal component analysis to MGG recordings, which were acquired in our case from ten normal human patients using a Superconducting QUantum Interference Device (SQUID) magnetometer. Both pre- and post-prandial recordings were acquired for each patient and 20 min of recordings (10 min of pre-prandial and 10 min of post-prandial data) were analysed for each patient. The mean percentage of ECA slow waves that were found to exhibit spikes of suspected ERA origin was 41% and 61% for pre- and post-prandial recordings, respectively, implying a 47% ERA increase post-prandially ($P < 0.0001$ at a 95% confidence level). The detection of ERA in humans is highly encouraging and points to the possible use of non-invasive ERA recordings as a valuable tool for the study of human gastric disorders.

(Some figures in this article are in colour only in the electronic version)

1. Introduction and background

The study of gastric and intestinal motility from bioelectric and biomagnetic recordings is of great clinical interest due to the proven relationship between gastrointestinal (GI) disorders

and abnormalities in the characteristics of gastric electrical activity (GEA). In mammals and humans, GEA consists of two distinct phenomena: an electrical control activity (ECA) that manifests itself as an electric slow wave and an electrical response activity (ERA) that is characterized by spiking potentials during the plateau phase of the ECA.

It was first shown by Bortoff *et al* (1981) that ECA propagation along the GI tract is mediated by the presence of both circular and longitudinal smooth muscle groups, which are highly coupled in the healthy state (Elden and Bortoff 1984). The gastric interstitial cells of Cajal (ICC) act as pacemaker cells and possess unique ionic conductances that trigger slow wave activity, whereas smooth muscle cells lack the basic mechanisms required to generate ECA. Instead, cells of the latter type respond to the depolarization and repolarization cycle imposed by the ICC network and regulate L-type Ca^{2+} currents which are also responsible for the contractile behaviour of the stomach (Horowitz *et al* 1999). In both animals and humans, the antral region of the stomach has the capability of a pacemaker which generates and drives ECA slow waves along the gastric corpus in the direction of the pylorus (Horiguchi *et al* 2001). The slow wave signal recorded by the electrogastrogram (EGG) consists of an upstroke followed by a plateau and then by a slow depolarization phase. In humans, the frequency of the recorded ECA signal is of approximately 3 cycles per minute (cpm).

From a theoretical perspective, it was proposed by Sarna *et al* that ECA can be modelled using a system of bidirectionally coupled relaxation oscillators (Sarna *et al* 1971, 1972a, 1972b). Within the framework provided by this formalism, ERA was later shown to correspond to a bifurcation solution to the set of higher order partial differential equations that describe the dynamics of this coupled gastric activation system (Glass and Mackey 1988, Britton 1986).

There is much clinical interest associated with the study of ECA patterns to diagnose gastrointestinal diseases. The presence of abnormal ECA propagation patterns was found to be associated with gastric outlet obstruction (Brzana *et al* 1998, Smith *et al* 2003), gastroparesis (Smith *et al* 2003), gastric myoelectrical dysrhythmia (Qian *et al* 2003), atrophy and hypertrophy (Bortoff and Sillin 1986), diabetic gastropathy (Koch 2001) and Chagas disease (Madrid *et al* 2004), although no statistically significant differences were found between normal and abnormal EGG-recorded ECA patterns for human cases of achalasia (Verhagen *et al* 1998) and dysmotility-like functional dyspepsia (Oba-Kuniyoshi *et al* 2004, van der Voort *et al* 2003).

2. Motivation and purpose

The two most important procedures for measuring and quantifying GEA are the electrogastrogram (EGG) and magnetogastrogram (MGG). The EGG signal was first recorded by Alvarez (1921) with a galvanometer, whereas the use of electrodes for this procedure was pioneered by Bozler (1945). Hamilton *et al* (1986) were the first to use EGG with the purpose of investigating gastric motility disturbances from recordings of ECA potentials in humans.

Many have questioned the reliability of EGG in recent years. In a study by Liang and Chen (1997), it was shown that the detectability of gastric slow wave propagation from cutaneous EGG is dependent on the thickness of the abdominal wall and on the propagation velocity of the serosal slow wave. Another disadvantage of this method which was pointed out, among others, by Bortolotti (1998) is that the practicality of using EGG to detect alterations in slow wave frequency due to tachy- and bradygastria remains problematic in spite of considerable recent progress to improve filtering and analysis methods for this clinical procedure. Reservations concerning the significance of EGG as a diagnosis tool were also expressed by Camilleri *et al* (1998), who indicated that the precise meaning of dysrhythmias, signal amplitude changes and

the duration of such abnormalities relative to gastric emptying as quantified by EGG remain to be clarified. In addition, the stability of EGG recordings is affected by a variety of artefacts, such as the overlap of the electrical activities of the colon and stomach in cutaneous EGG recordings (Amaris *et al* 2002).

In response to many of these concerns, two techniques dubbed magnetogastrography (MGG) and magnetoenterography (MENG) were pioneered in the late 1980s and early 1990s as non-invasive alternatives to EGG, the first one by Comani *et al* in 1989 (DiLuzio *et al* 1989, Comani *et al* 1996) and the second one by Staton, Richards and Bradshaw in 1993 (Staton *et al* 1993, Golzarian *et al* 1994, Richards *et al* 1995, Staton *et al* 1995, Bradshaw 1995). In 1997, Bradshaw *et al* showed that a high degree of correlation exists between the ECA frequency values determined using EGG and MGG (Bradshaw *et al* 1997). Whereas bioelectric fields depend on tissue permittivity and are therefore much attenuated by the multiple layers of electrical insulators of the abdominal walls and omentum, magnetic fields depend on the permeability of biological tissues, which is nearly equal to that of free space. Thus there are significant advantages to the use of MGG for clinical investigations as compared to EGG.

Thus far, ERA has only been detected in animals using EGG and the only human study available was performed with invasive serosal electrodes (Hotokezaka *et al* 1996). In 1995, Atanassova *et al* recorded spiking activity from anaesthesized dogs using implanted and cutaneous electrodes (Atanassova *et al* 1995a, 1995b). In 1999, Akin and Sun recorded the spike activity of the canine stomach using EGG (Akin and Sun 1999). These authors concluded that ERA in serosal recordings occupies the frequency range of 50–80 cpm and later proposed an analysis method to extract the motility information from the EGG signal in the frequency range of ERA (Akin and Sun 2002). In 2001, Wang *et al* investigated canine ERA using a blind source separation algorithm (Wang and Chen 2001, Wang *et al* 2004, 2005). An increasing number of studies point to the possible use of ERA to identify and study gastric diseases. A study by Ouyang *et al* involving electroacupuncture of the canine stomach used ERA to quantify the improvement of gastric emptying brought about by the procedure (Ouyang *et al* 2002). Another investigation by Garcia-Casado *et al* used spike potential recordings made using surface electrodes to investigate and monitor intestinal mechanical activity in dogs (Garcia-Casado *et al* 2005). Finally, Xu *et al* studied the effects of enhanced viscosity on canine gastric and intestinal motility from invasive ECA and ERA recordings (Xu *et al* 2005).

The purpose of this paper is to report the first non-invasive detection of ERA in humans and to show that significant differences in ERA patterns exist in pre- and post-prandial GEA. In addition, we demonstrate the application of principal component analysis (PCA) to magnetogastrographic recordings with the purpose of isolating and characterizing ERA patterns in the human stomach. In the following section, we describe our experimental set-up for acquiring MGG data using a Superconducting QUantum Interference Device (SQUID) magnetometer. We then proceed by outlining our PCA method and the manner in which we have applied it throughout our data analysis process. The proposed non-invasive detection of ERA is then discussed, followed by the statistical analysis of pre- and post-prandial ERA patterns recorded from ten healthy human patients.

3. Methods

MGG signals were recorded using a multichannel SQUID magnetometer (637i model, Tristan Inc., San Diego CA) that possesses a set of detection coils located at the bottom of an insulated dewar filled with liquid helium ($T \approx 4$ K). The detection coils are magnetically coupled to the SQUID coils; the latter convert magnetic flux incident on the detection coils to voltage signals

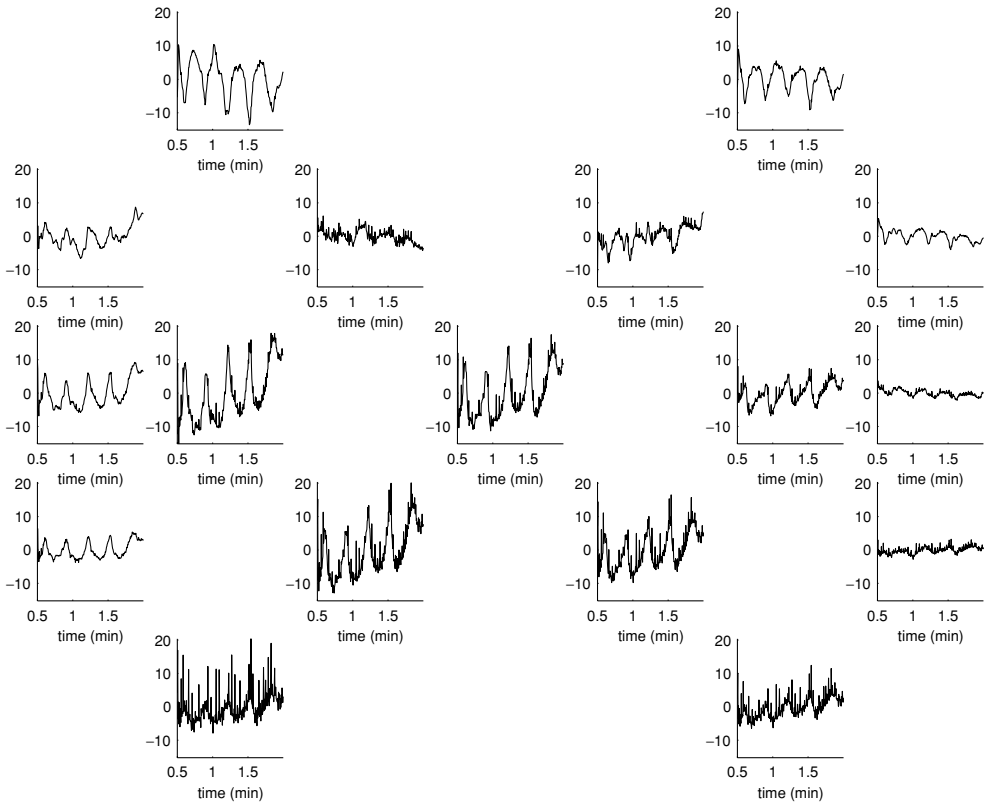

Figure 1. Sample raw MGG SQUID recording (B_z field component signals) acquired from a healthy human patient for a time interval of 1.5 min. Plots are shown in the approximate spatial arrangement of the SQUID magnetomer coils, which were positioned directly above the stomach of the subject. The upper edge of the input grid is located immediately below the diaphragm while each of its left and right extremities is approximately 3 cm away from the boundary of the body. The input grid has a diameter of 15 cm.

that are amplified and then acquired by a digital computer at the rate of 3 MHz. Detection coils are arranged in gradiometer format as a horizontal grid and 19 of them record the Cartesian component of the magnetic field that is normal with respect to the grid plane. At five of the 19 locations, the other two Cartesian components of the field are also measured.

Informed consent was obtained from ten healthy human volunteers and the study was approved by the Vanderbilt University Institutional Review Board. Each subject was positioned underneath the SQUID magnetometer inside a magnetically shielded room (Vacuumschmelze). Volunteers were asked to suspend respiration and lie quietly for a period of at least one minute during each recording. For each recording, the magnetometer was oriented such that the coils measuring the $\hat{\mathbf{x}}$ and $\hat{\mathbf{y}}$ components of the signal tangential to the body surface were oriented in the sagittal and horizontal planes, and the coil measuring the $\hat{\mathbf{z}}$ component normal to the body surface was oriented in the frontal plane. Sample plots of the MGG signals recorded from one healthy subject are presented in figure 1.

We have employed principal component analysis (PCA) (Johnson and Wichern 1988, Rencher 2002, Everitt and Dunn 1992, Harris 1975a) to reduce the dimensionality of our acquired MGG recordings. Originally introduced independently by Pearson (1901) and by

Hotelling (1933), PCA is a multivariate analysis technique that attempts to describe the variation of a set of multivariate data in terms of a set of uncorrelated variables each of which is a particular linear combination of the original variables (Everitt and Dunn 1992). In the present case, the recorded MGG signal includes not only the gastric ECA and ERA, but also other underlying variables that can be considered, in our case, to be artefacts due to respiration, cardiac activity and to the rest of the GI tract (duodenum, small and large intestine). Thus each computed principal component (PC) of the MGG observation set is a linear combination of the underlying variables in that set. Letting x_k represent one of these original n variables ($k = 1, \ldots, n$), the ith PC y_i can be formally defined as

$$y_i = \sum_{k=1}^{n} \alpha_{ik} x_k, \tag{1}$$

where α_{ik} are the linear coefficients (weights) assigned to each variable x_k for the ith PC y_i. In matrix notation, we have

$$\boldsymbol{x} = (x_1, x_2, \ldots, x_n) \tag{2}$$

$$\boldsymbol{\alpha}_i^T = (\alpha_{i1}, \alpha_{i2}, \ldots, \alpha_{in})^T \tag{3}$$

where $\boldsymbol{\alpha}_i^T$ denotes the transpose of the column matrix $\boldsymbol{\alpha}_i$. The definition of y_i can now be written simply as

$$y_i = \boldsymbol{\alpha}_i^T \boldsymbol{x}. \tag{4}$$

In PCA, the ith PC is that linear combination $\boldsymbol{\alpha}_i^T \boldsymbol{x}$ which maximizes the value of the variance $\mathrm{var}(y_i)$ subject to the orthonormality constraint specified by

$$\boldsymbol{\alpha}_i^T \boldsymbol{\alpha}_j = \delta_{ij}, \tag{5}$$

where δ_{ij} is the usual Kronecker delta-function. The variance is computed from

$$\mathrm{var}(y_i) = \mathrm{var}\left(\boldsymbol{\alpha}_i^T \boldsymbol{x}\right) \tag{6}$$

$$= \boldsymbol{\alpha}_i^T \boldsymbol{S} \boldsymbol{\alpha}_i, \tag{7}$$

where $\boldsymbol{S}$ is the variance–covariance matrix of the original variables. The optimization technique of Lagrange multipliers (Morisson 1967, Chatfield and Collins 1980) is applied in our approach to maximize the variance of each PC, which leads to the calculation of the eigenvectors of $\boldsymbol{S}$. These eigenvectors correspond to the eigenvalues of the variance–covariance matrix arranged in descending order according to their magnitude; thus the first PC can be interpreted as that linear combination of the original variables which maximally discriminates among a set of subjects. Z scores, defined as the data formed by transforming the original data into the space of the PCs, are also computed. An important statistic associated with PCA is Hotelling's T^2 statistic, which provides a measure of the multivariate distance of each observation from the centre of the data set. In our computational approach, in addition to the PCs, we also compute Z scores, the eigenvalues of the covariance matrix as well as Hotelling's T^2 statistic for each time data point.

After computing the PCs of an MGG data set, the so-called labelling problem of PCA must be addressed. This problem can be defined as the 'task of finding substantive interpretations of some set of hypothetical latent variables which have been derived through PCA' (Harris 1975b). In the case at hand, this translates into the challenge of associating one of the computed PCs with the gastric signal, which constitutes in this case the latent variable of interest. For the present study, the labelling problem was addressed using a visual analysis of the PCs that sought to identify the particular PC whose waveform best matched the gastric ECA waveform,

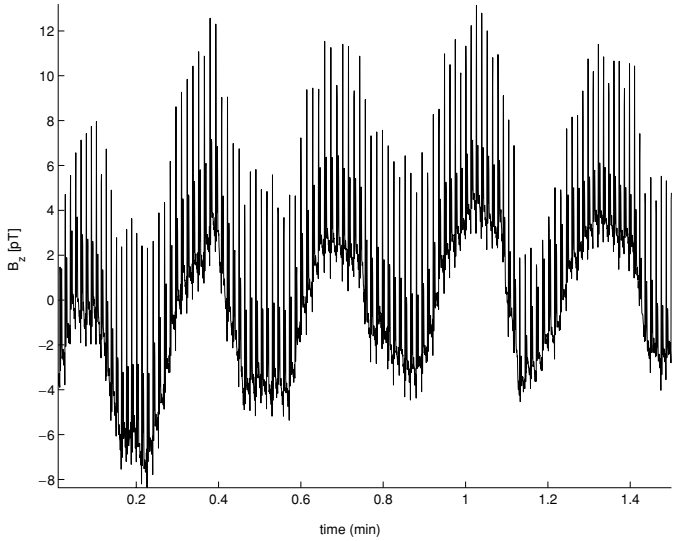

Figure 2. Selected gastric PC computed from the information provided by the signals in figure 1. The PC exhibits the characteristic waveform of ECA at a dominant frequency of 3 cpm.

which has a distinct frequency of 3 cpm. In most cases—including the example illustrated in our figures—the gastric PC was found to be among the first five PCs that accounted for the highest percentage of the variance in the recorded signals. We found this to be the case because the gastric signal is relatively strong compared to other components of biological origin and because it was superseded, in most cases, only by motion artefact signals. For the data set in figure 1, the selected PC is displayed in figure 2. As an aid to the decision process concerning the optimal PC to select, the power spectral density (PSD) of each PC was computed using the classical fast Fourier transform (FFT) and analysed visually, thus providing a time–frequency representation of the MGG data. The frequency spectrum of the PC in figure 2 is shown in figure 3.

After selecting a suitable PC, the signal provided by the chosen PC was processed for further analysis. First, linear detrending was applied to eliminate short-lived data trends due to extraneous causes, thus ensuring that low-frequency noise was eliminated. Then, a number of bandpass, second-order Butterworth filters were designed. The Butterworth filter is maximally flat in the pass-band and monotonic overall, which reduces the effect of pass-band ripples in the signal to a minimum. These types of filter sacrifices roll off steepness for monotonicity in the pass- and stop-bands. To generate each filter, z-transform coefficients were created for a lowpass digital Butterworth filter of order n with user-specified cutoff frequencies for each filter. Filter coefficients are specified in our approach in two rows a and b of length $n+1$, with coefficients listed in descending power of z:

$$H(z) = \frac{A(z)}{B(z)} \tag{8}$$

$$= \frac{b(1) + b(2)\frac{1}{z} + \cdots + b(n+1)\frac{1}{z^n}}{1 + a(2)\frac{1}{z} + \cdots + a(n+1)\frac{1}{z^n}}. \tag{9}$$

These coefficients are then used to filter the PC data in the forward and reverse directions for zero-phase filtering. After filtering in the reverse direction, our algorithm reverses the filtered sequence and runs it back through the filter; the resulting sequence has precisely zero-phase

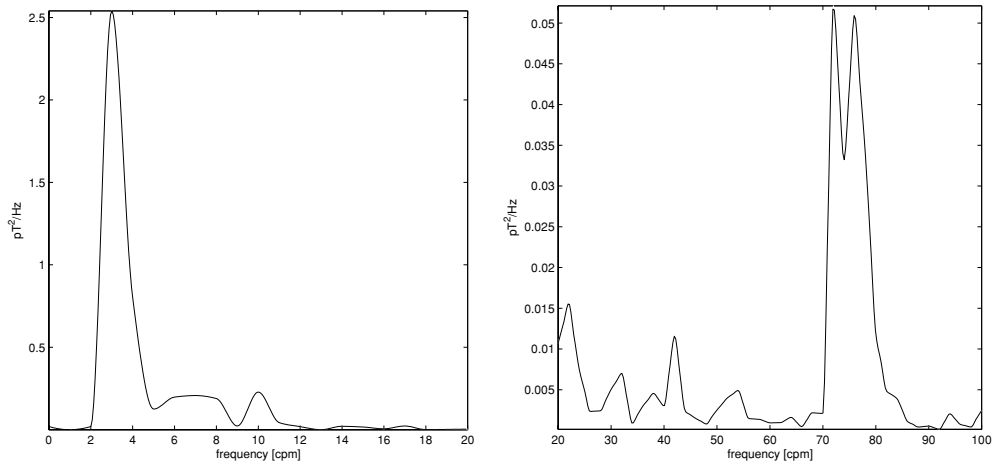

Figure 3. Frequency spectrum of the gastric PC in figure 2: (A) 1–20 cpm and (B) 20–100 cpm. The spectral energy present in the range 2–4 cpm corresponds to the gastric signal, whereas the peaks at 70–80 cpm is due to the cardiac artefact. A visual comparison of the ranges displayed on the vertical axes of the two plots (A) and (B) reveals that the gastric ECA signal is by far much stronger than both the respiration and cardiac artefacts. The power value associated with the highest peak in the frequency spectrum for the interval 100–500 cpm was found to be about 5×10^{-6} pT^2 Hz^{-1}, which is significantly lower than both (A) and (B); this demonstrates that high-frequency components in this range contribute very little to the signal; for this reason, the associated plot for the interval 100–500 cpm is not reproduced for brevity.

distortion and double the filter order. In addition, our algorithm attempts to minimize startup transients by adjusting initial conditions to match the dc component of the signal and by prepending several filter lengths of a flipped, reflected copy of the input signal.

4. Results and discussion

The cutoff frequencies used for our analysis and the resulting filtered waveforms obtained from the processing of the PC in figure 2 are presented in figure 4, where plots of magnetically recorded ECA and ERA are shown. It is well known that the ECG and MCG signals due to the human heart have characteristic components that are spread in a wide range of frequencies (Cohen 1988). Thus, unavoidably, although the dominant frequency of the cardiac signal is around 75 cpm for the example in figure 4, the frequency ranges of ERA and MGG must overlap at least partially. For this reason, we have chosen to display both signals using the method of figure 4(C), where the cutoff frequencies for the Butterworth filter were 60–100 cpm. In that figure, the cardiac waveform can be seen in the time interval between 0.45–0.80 min. However, another signal is also present in figure 4(C); this signal is both qualitatively and quantitatively different from the cardiac MCG signal and why this is the case is explained both below and by the analysis provided in figure 5.

(1) The amplitude of the second signal identified in figure 4(C) (i.e., the non-cardiac signal corresponding to the signal in figure 5(C)) is twice as high as that of the MCG signal. The latter signal remained approximately constant throughout the entire analysed time segment because the human subject lay still and did not move throughout the data acquisition process.

(2) The waveform of the second identified signal differs categorically from the MCG waveform (see figure 5).

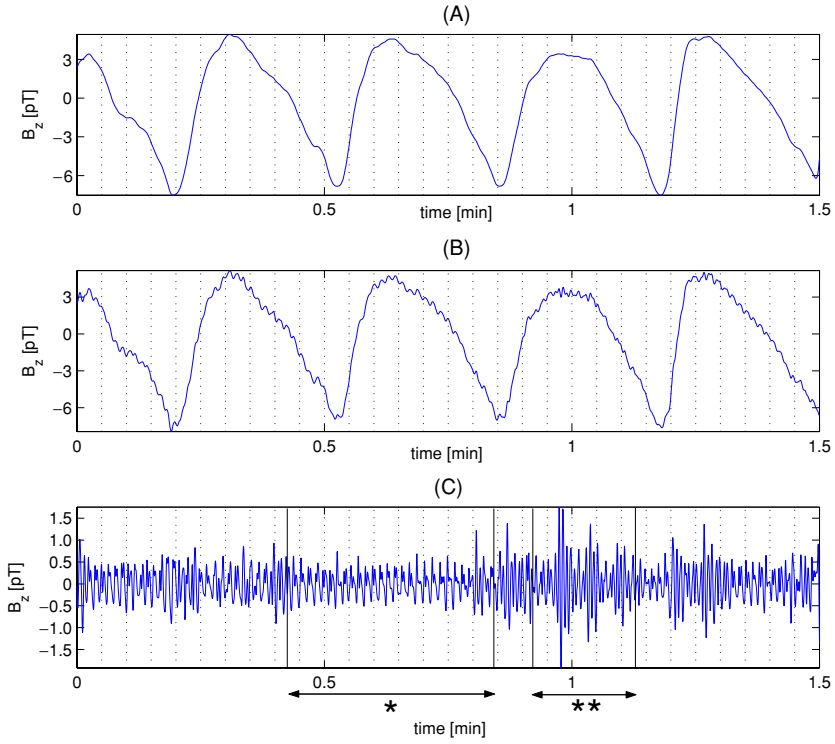

Figure 4. Human MGG and MCG recordings indicating the possible presence of ERA. Vertical grids are provided for convenience to emphasize the relationships that exist between the three waveforms. (A) gastric ECA waveform obtained from the gastric PC using a Butterworth filter with cutoff frequencies 1.8–40 cpm. (B) Superimposed gastric (ECA and ERA) and cardiac (magnetocardiogram—MCG) signals obtained by applying a Butterworth filter with cutoff frequencies of 1.8–100 cpm to the PC. (C) Superimposed gastric ERA and cardiac MCG signals obtained by applying a Butterworth filter with frequencies 60–100 cpm. The characteristic shape of the MCG signal is more evident throughout time segment 0.45–0.80 min, while the suspected ERA signal can be distinguished within time segments 0.20–0.45, 0.85–1.15 and 1.2–1.3 min. It can be noted that ERA has a higher amplitude and a lower frequency than the MCG signal and that it appears only during the plateau phase (i.e., after the beginning) of the associated ECA wave. Signals plotted within time intervals * and ** (delineated by vertical bars and horizontal arrows) are drawn separately and discussed further in figure 5.

(3) The non-cardiac signal was identified in the frequency range of 60–100 cpm, i.e., in approximately the same frequency range where ERA had been detected in animals (see, for example, Atanassova *et al* (1995a), Akin and Sun (1999)).

(4) Most importantly, the non-cardiac signal in figure 4(C) is seen only during the plateau phase of the corresponding ECA waveform in figure 4(A). This can be demonstrated by analysing time segments 0.20–0.45 min, 0.85–1.15 min and 1.2–1.3 min, where it is clear that the second identified signal appears on the plateau of the ECA wave. Thus the non-cardiac signal satisfies the properties of the ERA signal previously observed in canines and felines by a plethora of other GI researchers (Atanassova *et al* 1995a, Akin and Sun 1999, Wang and Chen 2001, Wang *et al* 2004). It is reasonable to assume that human ERA would be seen in about the same frequency range because the depolarization and contractile mechanisms of the gastric muscles that are responsible for ERA are very similar for both humans and animals.

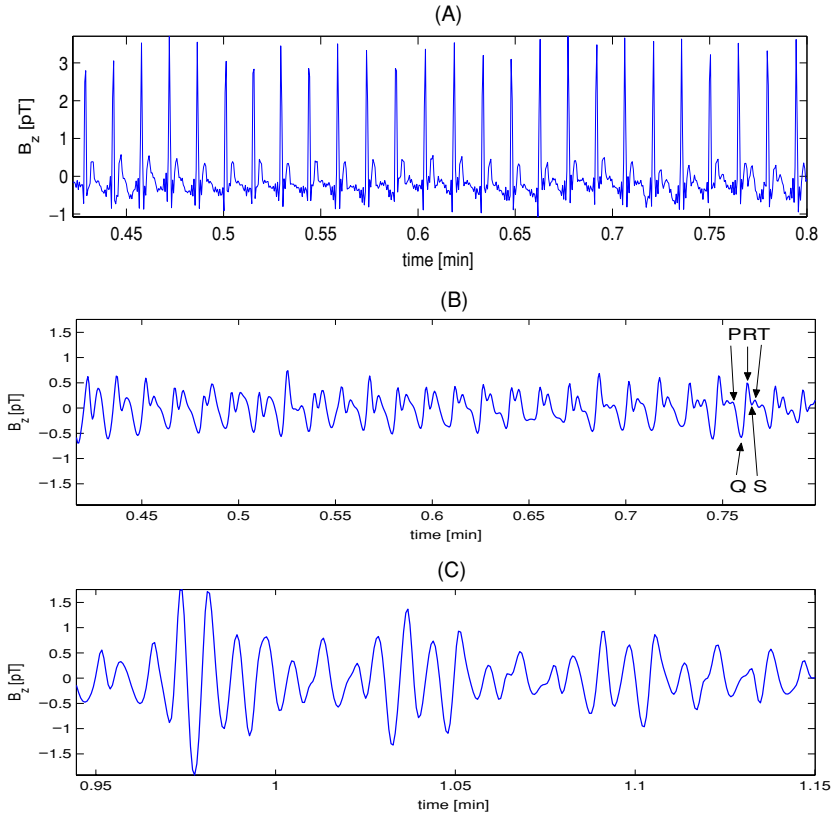

Figure 5. MCG (A), (B) and suspected ERA (C) waveforms isolated from figure 4(C). Time interval indications are identical to those in figure 4; note that the time scale in (A) and (B) differs from that in (C) because two different time intervals are displayed; i.e., (A) and (B) correspond to * in figure 4 while (C) corresponds to ** in figure 4. Vertical scale intervals are the same in both (B) and (C) to emphasize the difference in magnitude between the MCG and ERA signals. In (A), the *unfiltered* cardiac PC is shown; because no filter was applied there, the magnitude of the signal is higher than in (B), where the *filtered* MCG signal for the same time period in (A) is nevertheless still identifiable; the P, Q, R, S and T waves that are characteristic of cardiac activity are labelled for a sample MCG interval. In (C), the ERA waveform is of greater magnitude and does not exhibit MCG characteristics. The fact that the MCG and ERA are out of phase with each other is indicated by the presence of an oscillating envelope associated with the ERA signal, indicating again two distinct generating sources for the two phenomena.

(5) The second observed signal cannot be due to small or large intestine activities because the frequency ranges of these two types of electrical activity are far below the frequency range investigated here (i.e., 10–15 cpm for the small intestine and 8–12 cpm for the large intestine). In addition, skeletal muscle activity exhibits frequencies above the frequency range of 60–100 cpm investigated here and neither intestinal nor muscular activity are time-locked with the plateau phase of the ECA cycle.

In view of the reasons enumerated above, we conclude that the non-cardiac signal in figure 4(C) is generated by the ERA signal from the human stomach. This figure provides an example of what motivates our belief that we detected ERA from the MGG signal. Because our subjects lay still throughout the data acquisition process, there is no reason to consider the possibility of abrupt changes in the characteristics of the MCG signal for the time periods analysed. One might argue, however, that the presence of the non-cardiac signal on the plateau

Table 1. ERA analysis results for pre- and post-prandial human data (pre and post). Percentage differences were computed according to the formula (post–pre) × 100/pre.

	ECA waves with ERA spikes (%)		
Subject	Pre-prandial	Post-prandial	Difference (%)
1	28	47	68
2	30	50	67
3	36	54	50
4	38	63	66
5	39	61	56
6	40	67	68
7	46	62	35
8	46	63	37
9	52	67	29
10	56	72	29
Mean	41	61	47

phase of the ECA wave in figure 4 (point (4) above) is due to mere coincidence. In our analysis approach, however, this possibility was refuted in light of a statistical test applied to the ten human MGG data sets used in our study. This test was applied as follows. First, a computer-based analysis identical to that in figures 4(A)–(C) was conducted for every human data set used in this study. Then, for each slow wave detected in a data set (figure 4(A)), the associated plot analogous to that in figure 4(C) was analysed and every non-cardiac signal detected using the analysis above was subjected to criteria (1), (2) and (3) above. It was then found that, when the non-cardiac signal fulfilled all these three criteria, it also fulfilled criterion (4) above in more than 19 out of 20 cases (confidence level $>95\%$). Thus it is statistically reasonable to conclude that the appearance of our non-cardiac signal only during the plateau phase of the ECA is not a coincidence and that the signal is human ERA.

Post-prandial changes in ECA patterns have been investigated by a number of authors. Terasaka *et al* was among the first to show that that cellular coupling decreases post-prandially (Terasaka *et al* 1989). Post-prandial changes in electrical control activity that are recordable from serosal and cutaneous EGG recordings have been investigated, among others, by Lin *et al* (2000). Prompted to investigate this phenomenon by the controversial interpretations that have been given to the post-prandial increase in the dominant power of the EGG, these researchers concluded that exogenous stimulation—such as water ingestion—may change ECA amplitudes that are reflected in the EGG.

To study the effect of eating upon ERA characteristics, the analysis methods presented in the previous section were applied to the MGG data acquired from ten healthy human volunteers. Both pre- and post-prandial recordings were acquired for each patient and 20 min of recordings (10 min of pre- and 10 min of post-prandial data) were analysed for each patient. After acquiring pre-prandial data, subjects were given a standard turkey sandwich and 300 ml of water, whereafter post-prandial data were acquired.

The results of our data analysis are summarized in table 1. For each patient, the number of ECA waves was counted and the percentage of those waves that exhibited what we suspect to be ERA patterns detectable using our algorithm was also computed. The fact that the percentage of ECA waves with ERA activity is different from subject to subject is an indicator of inter-patient anatomical and physiological variability as well as other factors such as different signal-to-noise ratios for each experiment, small experimental set-up differences, etc. Nevertheless, as a result of applying a two-tailed paired t test, a statistically significant difference between

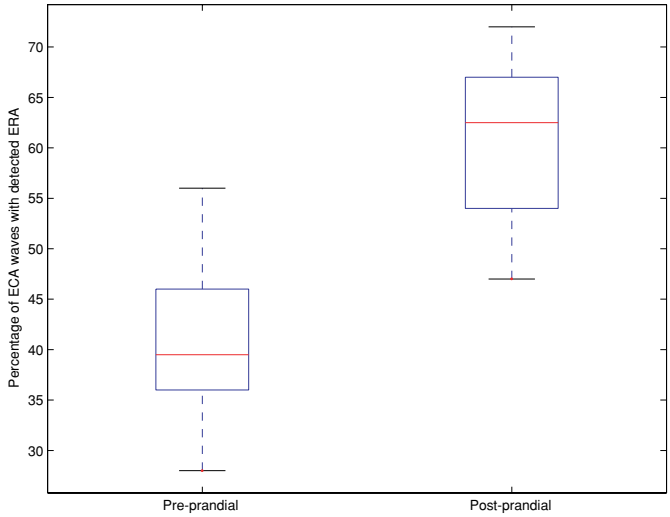

Figure 6. Box plot of post-prandial percentages of ECA waves exhibiting ERA versus similar pre-prandial percentages. Horizontal lines indicate the mean, first and third quartiles and ranges of the percentage values (no outliers were found). The statistical difference between the means of the two quantities plotted indicates that eating leads to a statistical increase in ERA ($p < 0.0001$).

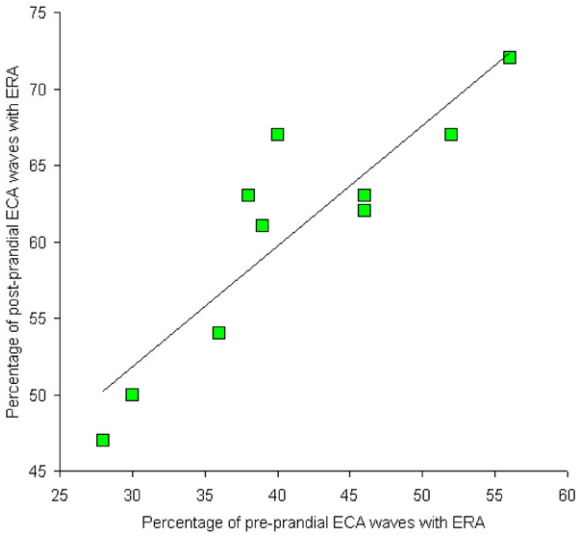

Figure 7. Plot of post-prandial percentages of ECA waves believed to exhibit ERA versus similar pre-prandial percentages. The line of best fit in the least-squares sense is also displayed. The fit to the data indicates that a linear increase in ERA amplitude is associated with eating.

pre- and post-prandial ERA recordings was found ($p < 0.0001$). We believe this to be evidence that, as a result of eating, the amplitude of ERA increases by approximately one-half of its pre-prandial value in normal humans. This conclusion is supported by the box plot in figure 6, where it can be seen that a statistical difference exists between pre- and post-prandial averages of ECA wave percentages with exhibited ERA.

A simple plot of the quantities in the third column of the table (post-prandial percentage) versus those in the second table (pre-prandial percentage) is shown in figure 7. The least-squares line of best fit was computed using a nonlinear optimization algorithm. The result of applying this technique shows that a linear relationship between the two quantities (pre- and post-prandial percentages) is quite suitable. What this indicates is that the amplitude of ERA in the human stomach increases linearly from pre- to post-prandial recordings by approximately 50%. Whereas this is expected on physiological grounds because ERA is associated with the contractile behaviour of the stomach (which increases post-prandially during digestion), this is the first study to report and quantify this increase in humans. Thus these results may represent an independent confirmation of the close relationship of direct dependence between ERA and the contractile activity of the gastric smooth muscle using the novel biomagnetic method of investigation. Moreover, the fact that this result could be obtained from our analysis without having treated it as an assumption throughout our investigation is an indicator in favour of biomagnetic method reliability.

The ERA patterns detected using our algorithm were found to exhibit a dominating frequency of 61.2 $\pm$ 2.4 cpm (mean $\pm$ SE, where the standard error SE of the sample was computed based on its standard deviation $\hat{\sigma}$ using the formula SE = $\hat{\sigma}/\sqrt{n}$ where $n = 10$ is the sample size). This value differs significantly from the dominating frequency of the cardiac signal, which was found to be 77.6 $\pm$ 1.7 cpm (mean $\pm$ SE). What this may imply is that there is relatively little overlap between the frequency contents of the two signals, which is of course benefic from the standpoint of isolating and studying ECA during the analysis process.

An important issue to note at this point is that, since this is the first reported ERA detection from non-invasive MGG recordings, some type of independent validation of the results presented here must be obtained by means of a highly reliable method such as invasive serosal recordings from humans. Although such recordings are not available in our case, we can state confidently that we have detected and analysed a type of signal that is time-locked with the plateau phase of ECA and that we strongly believe to be a human ERA signal. To fully ascertain the validity of our claim, a future correlation study involving direct serosal or mucosal electrode recordings—which has been done before and is therefore a trusted method—and MGG recordings is necessary.

5. Conclusions and future research

In conclusion, by means of a PCA of non-invasively acquired MGG signals, we have detected a biological signal with characteristics that strongly resemble those of gastric ERA in humans. By analysing the frequency spectrum of the gastric PC, we found suspected human ERA in the frequency range of 60–100 cpm, as well as post-prandial increases in the contractile activity of the smooth gastric muscle. Our analysis technique opens a new avenue of investigation into the characterization of gastric diseases in man, including the possible future development of non-invasive methods of diagnosis that could potentially differentiate between gastric diseases of neurological and muscular origin based on the principal component analysis of ERA recordings.

Acknowledgments

The authors are grateful to A J Pullan and L K Cheng of the Bioengineering Institute at the University of Auckland for their careful reading of the manuscript and for their useful comments and suggestions. Michael R Gallucci of the Vanderbilt University Medical Center

also provided important suggestions. Funding was provided by the National Institute of Health, grant nos RO1 DK 58697 and R01 DK 058197.

References

Akin A and Sun H H 1999 Time-frequency methods for detecting spike activity of stomach *Med. Biol. Eng. Comput.* **37** 381–90

Akin A and Sun H H 2002 Non-invasive gastric motility monitor: fast electrogastrogram (fEGG) *Physiol. Meas.* **23** 505–19

Alvarez W C 1921 The electrogastrogram and what it shows *J. Am. Med. Assoc.* **78** 1116–9

Amaris M A, Sanmiguel C P, Sadowski D C, Bowes K L and Mintchev M P 2002 Electrical activity from colon overlaps with normal gastric electrical activity in cutaneous recordings *Dig. Dis. Sci.* **47** 2480–5

Atanassova E, Daskalov I, Dotsinsky I, Christov I and Atanassova A 1995a Non-invasive electrogastrography part 1: correlation between the gastric electrical activity in dogs with implanted and cutaneous electrodes *Arch. Physiol. Biochem.* **103** 431–5

Atanassova E, Daskalov I, Dotsinsky I, Christov I and Atanassova A 1995b Non-invasive electrogastrography part 2: human electrogastrogram *Arch. Physiol. Biochem.* **103** 436–41

Bortoff A, Michaels D and Mistretta P 1981 Dominance of longitudinal muscle in propagation of intestinal slow waves *Am. J. Physiol.: Cell Physiol.* **240** C135–C147

Bortoff A and Sillin L F 1986 Changes in intercellular electrical coupling of smooth muscle accompanying atrophy and hypertrophy *Am. J. Physiol.: Cell Physiol.* **250** C292–C298

Bortolotti M 1998 Electrogastrography: a seductive promise, only partially kept *Am. J. Gastroenterol.* **93** 1791–4

Bozler E 1945 The action potentials of the stomach *Am. J. Physiol.* **144** 693–700

Bradshaw L A 1995 Measurement and modeling of gastrointestinal bioelectric and biomagnetic fields *PhD Dissertation* Vanderbilt University, Nashville TN

Bradshaw L A, Allos S H, Wikswo J P Jr and Richards W O 1997 Correlation and comparison of magnetic and electric detection of small intestinal electrical activity *Am. J. Physiol.: Gastrointest. Liver Physiol.* **272** G1159–G1167

Britton N F 1986 *Reaction–Diffusion Equations and Their Applications to Biology* (London: Academic)

Brzana R J, Koch K L and Bingaman S 1998 Gastric myoelectrical activity in patients with gastric outlet obstruction and idiopathic gastroparesis *Am. J. Gastroenterol.* **93** 1803–9

Camilleri M, Hasler W L, Parkman H P, Quigley E M M and Soffer E 1998 Measurement of gastrointestinal motility in the GI laboratory *Gastroenterology* **115** 747–62

Chatfield C and Collins A J 1980 *Introduction to Multivariate Analysis* (London: Chapman and Hall)

Cohen A 1988 *Biomedical Signal Processing* vol 2 (Boca Raton, FL: CRC Press) pp 121–4

Comani S, Conforto S, di Nuzzo D, Basile M, di Luzio S, Erné S N and Romani G L 1996 Non-invasive detection of gastric myoelectrical activity: comparison between results of magnetogastrography and electrogastrography in normal subjects *Phys. Med.* **12** 35–4

DiLuzio S, Comani S, Romani G L, Basile M, DelGratta C and Pizzella V 1989 A biomagnetic method for studying gastrointestinal activity *Nuovo Cimento* **11** 1853–9

Elden L and Bortoff A 1984 Electrical coupling of longitudinal and circular intestinal muscle *Am. J. Physiol.: Gastrointest. Liver Physiol.* **246** G618–G626

Everitt B S and Dunn G 1992 *Applied Multivariate Data Analysis* (New York: Oxford University Press) pp 45–64

Garcia-Casado J, Martinez-de-Juan J L and Ponce J L 2005 Noninvasive measurement and analysis of intestinal myoelectrical activity using surface electrodes *IEEE. Trans. Biomed. Eng.* **52** 983–91

Glass L and Mackey M C 1988 *From Clocks to Chaos: the Rhythms of Life* (Princeton, NJ: Princeton University Press)

Golzarian J, Staton D, Wikswo J P, Friedman R N and Richards W O 1994 Diagnosing intestinal ischemia using a noncontact superconducting quantum interference device *Am. J. Surg.* **167** 586–92

Hamilton J W, Bellahsene B E, Reichelderfer M, Webster J G and Bass P 1986 Human electrogastrograms: comparison of surface and mucosal recordings *Dig. Dis. Sci.* **31** 33–9

Harris R J 1975a *A Primer of Multivariate Statistics* (New York: Academic) pp 156–204

Harris R J 1975b *A Primer of Multivariate Statistics* (New York, NY: Academic) p 163

Horiguchi K, Semple G S A, Sanders K M and Ward S M 2001 Distribution of pacemaker function through the tunica muscularis of the canine gastric antrum *J. Physiol.* **537.1** 237–50

Horowitz B, Ward S M and Sanders K M 1999 Cellular and molecular basis for electrical rhythmicity in gastrointestinal muscles *Annu. Rev. Physiol.* **61** 19–43

Hotelling H 1933 Analysis of a complex of statistical variables into principal components *J. Educ. Psychol.* **24** 417–41

Hotokezaka M, Mentis E P and Schirmer B D 1996 Gastric myoelectric activity changes following open abdominal surgery in humans *Dig. Dis. Sci.* **41** 864–9

Johnson R A and Wichern D W 1988 *Applied Multivariate Statistical Analysis* (Englewood Cliffs, NJ: Prentice-Hall) pp 340–77

Koch K L 2001 Electrogastrography: physiological basis and clinical application in diabetic gastropathy *Diabetes Tech. Ther.* **3** 51–62

Liang J and Chen J D Z 1997 What can be measured from surface electrogastrography—computer simulations *Dig. Dis. Sci.* **42** 1331–43

Lin Z, Chen J D Z, Schirmer B D and McCallum R W 2000 Postprandial response of gastric slow waves: correlation of serosal recordings with the electrogastrogram *Dig. Dis. Sci.* **45** 645–51

Madrid A M, Quera R, Defilippi C, Defilippi C, Gil L C, Sapunar J and Henríquez A 2004 Gastrointestinal motility disturbances in chagas disease *Rev. Med. Chile* **132** 939–46

Morisson D F 1967 *Multivariate Statistical Methods* (New York: McGraw-Hill)

Oba-Kuniyoshi A S, Oliveira J A, Moraes E R and Troncon L E A 2004 Postprandial symptoms in dysmotility-like functional dyspepsia are not related to disturbances of gastric myoelectrical activity *Braz. J. Med. Biol. Res.* **37** 47–53

Ouyang H, Yin J, Wang Z S, Pasricha P J and Chen J D Z 2002 Electroacupuncture accelerates gastric emptying in association with changes in vagal activity *Am. J. Physiol. Gastrointest. Liver Physiol.* **282** G390–G396

Pearson K 1901 On lines and planes of closest fit to systems of points in space *Phil. Mag.* **2** 559–72

Qian L W, Pasricha P J and Chen J D Z 2003 Origins and patterns of spontaneous and drug-induced canine gastric myoelectrical dysrhythmia *Dig. Dis. Sci.* **48** 508–15

Quigley E M M 2000 Gastroduodenal motility *Curr. Opin. Gastroenterol.* **16** 479–88

Rencher A C 2002 *Methods of Multivariate Analysis* (New York: Wiley-Interscience) pp 380–407

Richards W O, Garrard C L, Allos S H, Bradshaw L A, Staton D J and Wikswo J P 1995 Noninvasive diagnosis of mesenteric ischemia using a SQUID magnetometer *Ann. Surg.* **221** 696–705

Sarna S K, Daniel E E and Kingma Y J 1971 Simulation of slow-wave electrical activity of small intestine *Am. J. Physiol.* **221** 166–75

Sarna S K, Daniel E E and Kingma Y J 1972a Simulation of the electric-control activity of the stomach by an array of relaxation oscillators *Dig. Dis. Sci.* **17** 299

Sarna S K, Daniel E E and Kingma Y J 1972b Premature control potentials in the dog stomach and in the gastric computer model *Am. J. Physiol.* **222** 1518–3

Smith D S, Williams C S and Ferris C D 2003 Diagnosis and treatment of chronic gastroparesis and chronic intestinal pseudo-obstruction *Gastroenterol. Clin. N. Am.* **32** 618

Staton D J, Golzarian J, Wikswo J P, Friedman R N and Richards W O 1993 SQUID magnetometer diagnosis of experimental small bowel ischemia *Proc 15th Annu. Int. Conf. IEEE EMBS* pp 1521–2

Staton D, Golzarian J, Wikswo J P, Friedman R N and Richards W O 1995 Measurements of small bowel electrical activity in vivo using a high-resolution SQUID magnetometer *Biomagnetism: Fundamental Research and Clinical Applications* (Boston, MA: Elsevier) pp 748–52

Terasaka D, Bortoff A and Sillin L F 1989 Postprandial changes in intestinal slow-wave propagation reflect a decrease in cell coupling *Am. J. Physiol.: Gastrointest. Liver Physiol.* **257** G463–G469

van der Voort I R, Osmanoglou E, Seybold M, Heymann-Mönnikes I, Tebbe J, Wiedenmann B, Klapp B F and Mönnikes H 2003 Electrogastrography as a diagnostic tool for delayed gastric emptying in functional dyspepsia and irritable bowel syndrome *Neurogastroenterol. Mot.* **15** 467–73

Verhagen M A M T, Samson M and Smout A J P M 1998 Gastric myoelectrical and antroduodenal motor activity in patients with achalasia *Neurogastroenterol. Mot.* **10** 211–8

Wang Z S and Chen J D Z 2001 Blind separation of slow waves and spikes from gastrointestinal myoelectrical recordings *IEEE Trans. Inf. Tech. Biomed.* **5** 133–7

Wang Z S, He Z and Chen J D Z 2004 Chaotic behavior of gastric migrating myoelectrical complex *IEEE Trans. Biomed. Eng.* **51** 1401–6

Wang Z S, He Z and Chen J D Z 2005 Robust time delay estimation of bioelectric signals using least absolute deviation neural network *IEEE Trans. Biomed. Eng.* **52** 454–62

Xu X, Brining D, Rafiq A, Hayes J and Chen J D Z 2005 Effects of enhanced viscosity on canine gastric and intestinal motility *J. Gastroenterol. Hepatol.* **20** 387–94